Journal of Power Sources 185 (2008) 1015–1021

Contents lists available at ScienceDirect

Journal of Power Sources

journal homepage: www.elsevier.com/locate/jpowsour

In situ analysis on water transport in a direct methanol fuel cell durability test

Yang Tian[a,b], Gongquan Sun[a,*], Qing Mao[a,b], Suli Wang[a], He Liu[a,b], Qin Xin[a,c]

[a] Dalian Institute of Chemical Physics, Chinese Academy of Sciences, 457 Zhongshan Road, Dalian 116023, China
[b] Graduate School of the Chinese Academy of Sciences, Beijing 100039, China
[c] State Key Laboratory of Catalysis, Dalian Institute of Chemical Physics, Chinese Academy of Sciences, Dalian 116023, China

ARTICLE INFO

Article history:
Received 3 July 2008
Received in revised form 29 August 2008
Accepted 29 August 2008
Available online 9 September 2008

Keywords:
Direct methanol fuel cell
Durability
Performance recovery
Water analysis
Cathode gas diffusion layer

ABSTRACT

In present work, a 600 h durability test and in situ measurements of water transport were carried out on a single direct methanol fuel cell (DMFC) at atmospheric pressure and 80 °C. Effect of water transport on the single cell performance was investigated in detail, which indicated that the accumulated water in the hydrophobic micropores of the cathode gas diffusion layer (GDL) aggravated the cathode flooding, and consequently led to a temporary and reversible degradation of the cell performance. Further investigation revealed that cathode flooding could be alleviated by blowing the cathode with dry air for 150 h at open circuit condition and the partially recovered cell performance within the durability could be obtained in consequence. Water analysis combined with the scanning electron microscopy (SEM), contact angle measurement and energy dispersive X-ray (EDX) was used to explore the characteristics of cathode GDL before and after the durability test. Results showed that the variation of the microstructure and hydrophobic properties for both sides of the cathode GDL is probably one of the inherent reasons for the irreversible degradation of the cell performance besides the electro-catalysts deterioration.

1. Introduction

Liquid-fed direct methanol fuel cell (DMFC) has received much attention as one of the promising power sources for portable electronic devices, electric vehicles and other mobile applications due to its high power density, environmental friendly and compact system design [1–3]. However, further development of DMFC is still prohibited by a number of significant technical hurdles, among which the durability of DMFC is one of the key challenges [4].

Many investigations have been made to find the reasons for DMFC deterioration during durability tests. Most of the researches focused on the degradation of key materials, such as the electro-catalysts and the proton exchange membrane. The agglomeration of electro-catalyst particles was believed to be one of the main reasons for the performance degradation [5–6]. Ruthenium crossover from anode through the membrane to cathode was reported as another key contributor in literatures [7–9]. The chemical aging of Nafion® membrane after single cell lifetime test was also responsible to the degradation of DMFC performance [6]. Moreover, further studies have been focused on the structural variation of membrane electrode assembly (MEA) in resent years. The negative effect of MEA delamination on DMFC durability was proposed [10–12] and the variation of F/C atomic ratio for the cathode gas diffusion layer (GDL) was also supposed to be correlated with the durability degradation [8].

In addition, Wang [13] indicated that water management and water crossover through the membrane is a significant factor affecting DMFC performance, as the accumulated water in the cathode not only decreases the oxygen/air transport efficiency, but also influences the electrode reaction kinetics. Thereafter, basing on Wang's study, follow-on works showed the effects of MEA structure on water crossing the membrane [14–16]. Xu et al. [14] claimed that the water-crossover flux through the membrane decreased slightly with the increase of polytetrafluoroethylene (PTFE) loading in the cathode backing layer (BL). Peled et al. [15] used a liquid–water barrier to minimize the water loss from the DMFC anode in their study. Liu et al. [16] designed a novel structure with a microporous layer basing on Nafion® 112 and obtained a relatively low net water transport coefficient. However, few works have been done on the variation of water-crossover flux from anode to cathode and its influence on cell performance during a DMFC durability test.

In this work, a 600 h durability test was implemented on a DMFC single cell at ambient pressure and 80 °C. A stage of 150 h "cathode blowing" with dry air at open circuit was inserted into the durability test. Furthermore, contributors to the collected water were obtained through theoretical analysis. Thereby the degraded and partially recovered cell performance during the whole durability test could be systematically illustrated by the varied water fluxes. In addition, the unrecoverable degradation of the cathode GDL was

* Corresponding author. Tel.: +86 411 84379063; fax: +86 411 84379063.
E-mail address: gqsun@dicp.ac.cn (G. Sun).

0378-7753/$ – see front matter © 2008 Elsevier B.V. All rights reserved.
doi:10.1016/j.jpowsour.2008.08.095

examined by contact angle measurement, SEM and EDX analysis before and after the 600 h potentiostatic test.

2. Experimental

2.1. MEA preparation

Pre-treatment of H^+-Nafion®-1135 (E.I. DuPont de Nemours and Company) membrane was accomplished by boiling successively in 3–5% H_2O_2 aqueous solution, deionized (DI) water, 0.5 mol L^{-1} H_2SO_4 aqueous solution, and then DI water again. Each step took 1 h.

For the anode, unsupported PtRu black (Johnson Matthey HiSpec 6000, Pt:Ru = 1:1 atomic ratio) was sonicated together with DI water and Nafion ionomer (DuPont) in an ice bath for 40 min to prepare the catalyst ink. Then it was painted onto a commercialized ELAT DS (E-TEK, Natick, MA) GDL to form the anode electrode with 7.4 mg PtRu cm^{-2}. Pt/C (Johnson Matthey HiSpec 9100, 60 wt.%) was chosen as the cathode electro-catalysts and the catalyst ink was prepared with the same method as the one described above. The cathode electrode with 2.1 mg Pt cm^{-2} was obtained by spraying the ink onto the pre-treated Nafion membrane. Content of Nafion ionomer (dry weight) in both catalyst layers was 15 wt.%.

As it was mentioned above, commercialized ELAT DS (E-TEK, Natick, MA) GDL was used as the anode GDL, while the cathode GDL was not prepared as the normal one. Carbon paste was prepared by introducing carbon powder (Vulcan, XC72R, Carbot Co.) into the mixture of terpineol (Sinopharm Chemical Reagent Co. Ltd.) and triton X-100 (Shenyang, China) and then experiencing a process of mechanical stir and sonication, which lasted for 1 h. Thereafter, PTFE dispersion (3F New Material Co. Ltd.) was added to the cooled carbon paste to obtain the cathode microporous layer (MPL) ink. The weight ratio of carbon powder, terpineol, triton X-100 and PTFE was 2.46:50:1:2.46. Screen printing technique was used to apply the MPL ink to the Toray carbon paper (TGP-H-060, Toray Industries Inc.). The cathode GDL with abundant solvent was dried in an air oven at 60 °C for 4 h and then sintered in muffle furnace at 340 °C for 0.5 h. Carbon loading on the cathode GDL was 1.2 mg cm^{-2}.

MEA with 4 cm^2 geometrical area was assembled into a single cell with stainless steel plates owning serpentine flow-field channels.

2.2. Single cell test

Over-all cell performance and durability behavior at const-voltage of 0.45 V were measured by using a Fuel Cell Test System (Arbin Instrument Corp.) at 80 °C. 0.5 mol L^{-1} methanol aqueous solution with a flow of 1 mL min^{-1} was supplied to the anode compartment, and dry air with a flow rate of 40 SCCM was fed to the cathode compartment.

Anode polarization curves were measured by EG&G PAR 273A potentionstat/galvanostat at 80 °C. Detailed experimental procedure was described in our previous work [17]. Furthermore, IR-corrected cathode polarization curves were obtained from the sum of the IR-corrected cell voltage and the IR-corrected anode potential. Methanol crossover at open circuit was carried out by using the same equipment and experimental mode as the anode polarization measurements. While in the measurement, humidified N_2 instead of H_2 with a flow rate of 50 SCCM at 70 °C was fed to the cathode, acting as the working electrode. As suggested by Lu et al. [18], the equivalent methanol crossover current density (i_{cross}) can be calculated from the following equation:

$$i_{cross} = i_{ocv}\left(1 - \frac{i}{i_{lim}}\right) \quad (1)$$

where i_{cov} is the equivalent methanol crossover current density at open circuit, i the operating current density, i_{lim} the anode limiting current density, which could be gained from the anode polarization measurements.

Electrochemical area (ECA) of the anode catalyst layer was determined by CO-stripping test, whereas that of the cathode one was carried out by hydrogen-desorption measurement. For CO-stripping measurement, the cathode was fed with H_2, serving as both DHE and counter electrode. Humidified CO/Ar (5 vol.%) gas was first supplied to the anode at a constant electrode potential (0.1 V versus DHE) for 20 min and then it was replaced by high purity nitrogen lasting for another 20 min. Then the anode catalyst layer was scanned from 0.1 to 0.75 V (versus DHE) with a scanning rate of 20 mV s^{-1}. Thus ECA of the anode catalysts could be calculated from the integrated peak area of CO-adsorption. For hydrogen-desorption test, the anode was fed with humidified H_2 serving as DHE and counter electrode, while the cathode was supplied with DI water. CV curve was recorded within the potential range of 0–1.2 V (versus DHE) at a scanning rate of 20 mV s^{-1}. The integrated peak area of hydrogen-desorption (0.05–0.4 V versus DHE) was used to calculate the ECA of cathode catalysts.

2.3. Cathode water collection

A water trap filled with silica gel was located in an ice bath and connected to the cathode exit to collect the removal water. Water was collected intermittently at the 4th, 55th, 154th, 226th, 303rd, 411th, 522nd hours, respectively. And 2 h were kept for each collection. The weight of the collected water could be obtained by gravimetric analysis.

As proposed by Xu and Zhao [19], the cathode collected water includes three parts:

$$N_{H_2O} = N_{ORR} + N_{MOR} + N_{cross} \quad (2)$$

where N_{H_2O} is the total water flux collected from the cathode exit. N_{ORR} and N_{MOR} represent, respectively, the molar flux of water due to the oxygen reduction reaction (ORR) and crossover methanol oxidation reaction (MOR). It can be further expressed as below:

$$N_{ORR} = \frac{i}{2F} \quad (3)$$

$$N_{MOR} = \frac{i_c}{3F} \quad (4)$$

where i is the average current density during each period of water collection, and i_c the equivalent methanol-crossover current density measured just before the process of water collection.

N_{cross} as the total water flux from the anode to cathode can be calculated by subtracting N_{ORR} and N_{MOR} from the total water flux, and can be further expressed as the following equation [20]:

$$N_{cross} = \kappa\frac{i}{F} + D_{eff}\frac{\Delta c_{a-c}}{\delta_m} - \frac{K}{\mu}\Delta p_{c-a}\frac{\rho}{M_{H_2O}} \quad (5)$$

where $\kappa = i/F$ represents the water flux generated by electro-osmosis, $D_{eff}(\Delta c_{a-c})/(\delta_m)$ is the part of water flux produced by concentration gradient and the expression of $(K/\mu)\Delta p_{c-a}(\rho/M_{H_2O})$ is the part driven by hydraulic pressure difference from the cathode to anode.

2.4. Characterization of the cathode GDL

Contact angle measurements were performed on both sides of the fresh and faded cathode GDLs by using a contact angle system (JC2000C1, Powereach Instruments). Each sample was measured six times within different regions and the average value was taken as the contact angle in order to get a better accuracy.

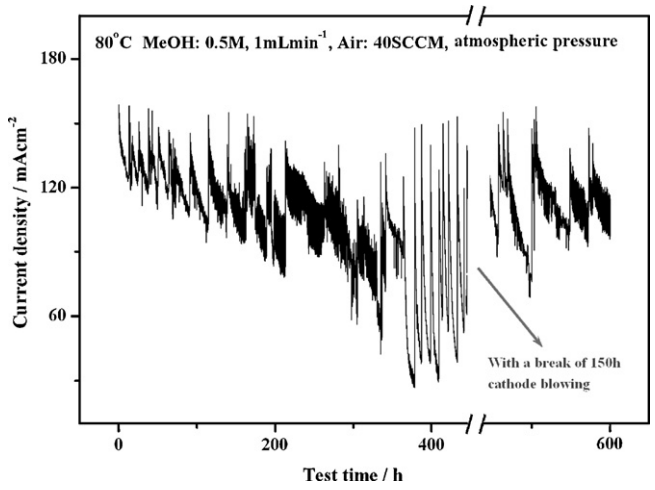

Fig. 1. Const-voltage discharge at 0.45 V.

The surface morphologies and structures of the cathode GDL before and after the durability test were observed by SEM (FEI QUANTA 200F). EDX (FEI QUANTA 200F) was developed on both sides of the fresh and faded cathode GDL to detect the F/C atomic ratio.

3. Results and discussion

3.1. Single cell performance

A 600 h const-voltage durability performance at 0.45 V for a single DMFC is shown in Fig. 1. According to the variation of discharge current density, the whole durability can be divided into the following three stages. The first one is during the period of 0–213 h, the second one is 213–446 h and the last one is from 446 h to the end. Moreover, a break of 150 h was conducted to the cell between the second and the third stage. During that period, both the inlet and the outlet of the anode were exposed to the air, and the cell cathode was fed by dry air with a flow rate of 10 SCCM in order to remove the residual water in the cathode. This process was so-called "cathode blowing".

IR-corrected polarization curves and the over-all cell performance measured at 0, 213, 446 and 600 h within the durability test are shown in Fig. 2. It can be observed that the anode performance at

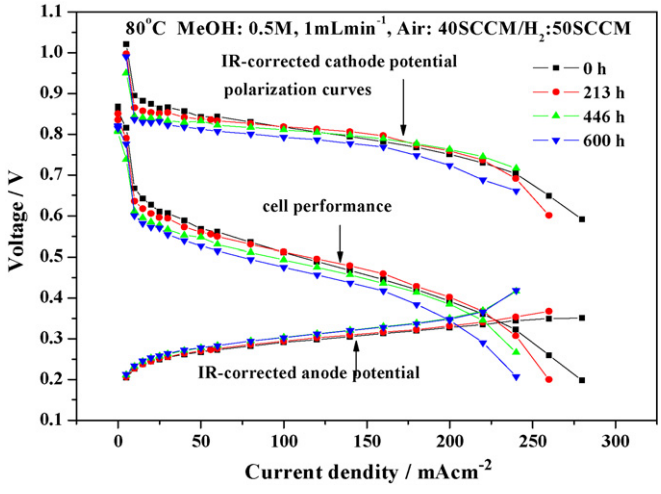

Fig. 2. Cell polarization curves at different time during the durability test.

Table 1
Comparison of current density (@0.45 V) for the over-all cell performance and durability performance.

Test time (h)	Over-all cell current density @0.45 V (mA cm^{-2})	Cell current density during the durability test (mA cm^{-2})	Difference of current densities @0.45 V (mA cm^{-2})
0	160	149[a]	11
213	160	95	65
446	140	65	75
600	120	107.5	12.5

[a] This value is obtained at 1 h.

213 h is a little worse than that at 0 h. However, it is obviously better than at 446 and 600 h, where the anode performance remains stable. For the cathode performance, it decreases continuously as the testing time goes on. But no distinct deterioration appears until the end of the durability test, where remarkable cathode degradation emerges.

In order to further compare the variation difference between the over-all cell performance and the durability performance, detailed current densities (@ 0.45 V) at 0, 213, 446 and 600 h were listed in Table 1. As revealed in Table 1, the cell performance tested in the *I–V* mode is always higher than that in the durability test. Additionally, the performance difference enlarges from 11 mA cm^{-2} of the beginning continuously to 75 mA cm^{-2}, when "cathode blowing" happens. Thereafter, the difference decreases to 12.5 mA cm^{-2} at the end of the 600 h durability test, which is still higher than 11 mA cm^{-2}. Thus, we can conclude safely that the cell performance degradation contains both reversible and irreversible degradation in the durability test.

3.2. Systematic analysis on cathode water during the durability test

As indicated by Eickes et al. [21], accumulation of liquid water in the cathode catalytic layer and cathode GDL is one of the most important reasons for the reversible performance-loss. In this paper, it can be confirmed by the correlation of the durability performance and the over-all cell performance. Firstly, if the significantly decreased durability performance in the second stage is caused by the anode performance degradation completely, the durability performance would not recover so much after the "cathode blowing" as shown in Fig. 2, as the anode polarization curve in the beginning of the last stage is even worse than the one in the beginning of the second stage. Secondly, the cathode performance keeps nearly the same at 213 and 446 h, which means no evident degradation of the cathode electro-catalysts appeared during this period. Therefore, it cannot lead to the serious attenuation of the durability performance either. Thus, the sharply deteriorated durability from 213 to 446 h should be attributed to the temporary and reversible degradation caused by "cathode flooding", which could be alleviated by "cathode blowing" and was once reported by Pasaogullari and Wang [22]. In addition, the recovery of the durability performance after "cathode blowing" confirms the reason for the recoverable degradation of the cell performance.

Fig. 3 shows water flux pouring out from the cathode outlet and its contributors at different period of time during the durability test. The amount of water collected from the cathode outlet shows a decreased tendency in general. It decreases from about 280 mg h^{-1} cm^{-2} in the beginning to 245 mg h^{-1} cm^{-2} in the last measurement. For the three parts, water-crossover flux from anode to cathode is the main contributor, which takes up about 80% and owns a similar variation tendency with the total water flux. Furthermore, as revealed in Fig. 3, water generated from MOR is always the smallest contributor during the whole testing process

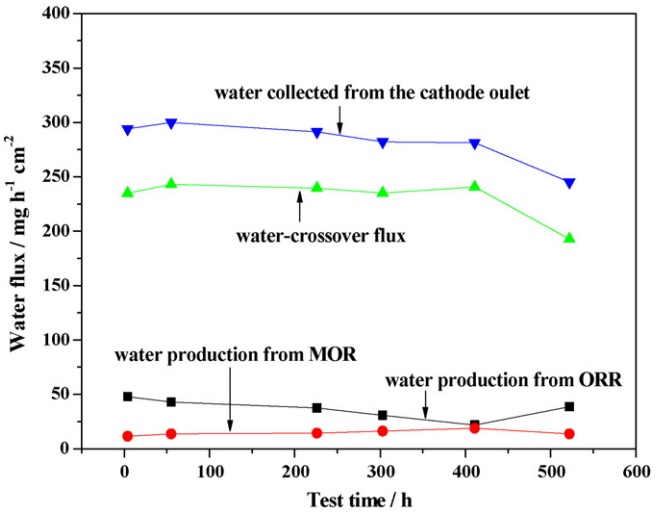

Fig. 3. Contributors to the water collected in the cathode outlet at different time during the durability test.

and has a completely reversed variation tendency with the one from ORR. Water produced from ORR reduces continuously with the decrease of the current density, whereas water generated from MOR increases at the meanwhile.

Contributors to water flux crossing over the membrane from anode to cathode are shown in Fig. 4. As it was reported by Nakagawa et al. [23], the electro-osmosis drag coefficient κ for Nafion electrolyte in contact with liquid water is a function of temperature, which can be fitted as

$$\kappa = 1.6767 + 0.0155\,T + 8.9074 \times 10^{-5} T^2, \quad T \text{ is the temperature in } ^\circ\text{C} \tag{6}$$

Though it may have some difference with the real value in our work, no influence will be produced when only observing the variation tendency of electro-osmotic water and diffusive water (generated by both concentration gradient and counter hydraulic permeation). Thus the calculated value 3.5 is introduced as the electro-osmosis drag coefficient to gain water dragged by electro-osmosis during the durability test. Because electro-osmotic water is in proportion to current density [24], it varies consistently with the cell durability performance, which can be observed by contrasting Figs. 1 and 4. Moreover, it is worth noting that the electro-osmotic water flux is the bigger contributor to the total water-crossover flux, when compared with the diffusive water flux. The diffusive water flux is $-99\,\text{mg}\,\text{h}^{-1}\,\text{cm}^{-2}$ for the first time water was collected. Thereafter it reaches $-22\,\text{mg}\,\text{h}^{-1}\,\text{cm}^{-2}$ after 226 h operation. It exceeds zero at 303 h and touches its peak value of $89\,\text{mg}\,\text{h}^{-1}\,\text{cm}^{-2}$ at 411 h. Finally, it decreases to below zero after the "cathode blowing" process is performed on the cell cathode. The negative diffusion flux here implies the transport direction of diffusive water is from cathode to anode.

In the beginning of the durability test, current densities are relatively high as shown in Fig. 1, which leads to large water flux driven by electro-osmosis from anode to cathode and consequently high water activity on the interface of membrane and cathode catalyst layer as indicated by Ren and Gottesfeld [25]. Thus water flux generated by concentration gradient from anode to cathode will be small. In addition, no residual water is accumulated in the GDL's hydrophobic micropores in the beginning. So the capillary force on the gas/liquid interface of the GDL's hydrophobic micropores is large [18], which leads to high hydraulic pressure and large water cross-over flux from cathode to anode by counter hydraulic permeation. Therefore, the large diffusive water flux from the cathode to

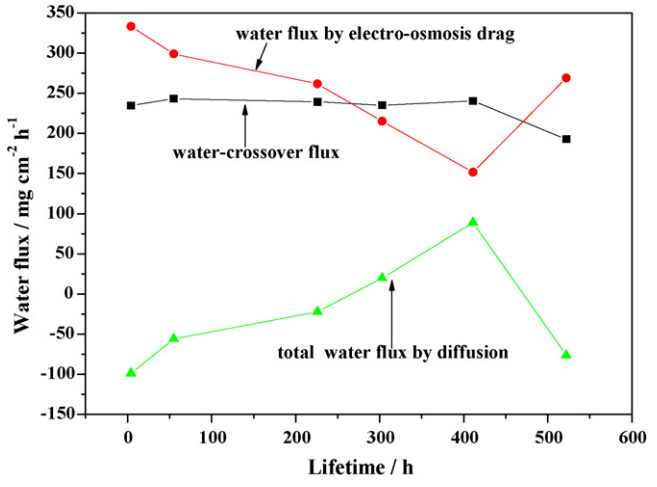

Fig. 4. Contributors to the water-crossover flux at different time during the durability test.

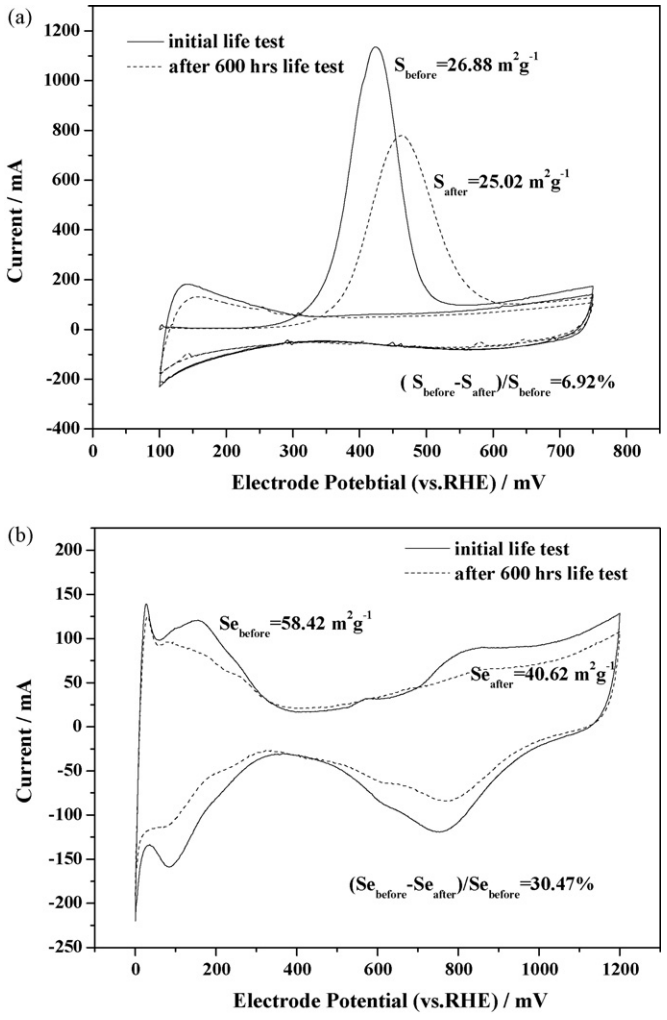

Fig. 5. (a) CO-stripping curves of the anode catalyst layer and (b) CV curves of the cathode catalyst layer before and after the durability test.

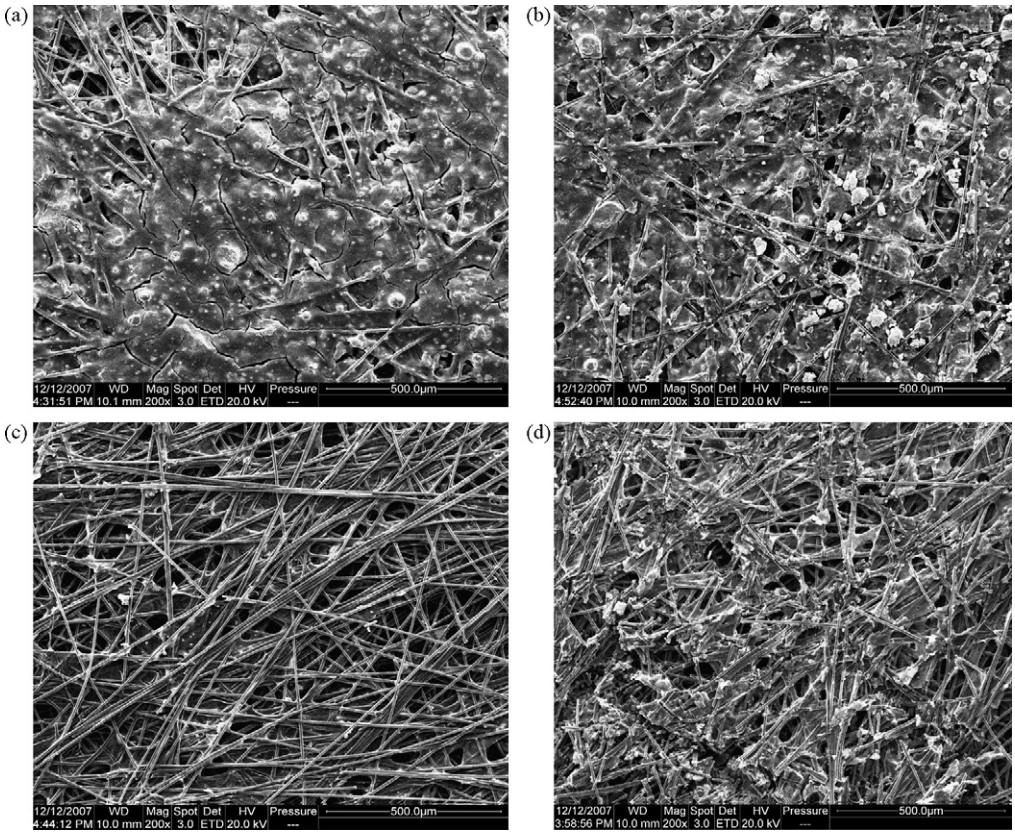

Fig. 6. SEM images for the fresh and faded cathode gas diffusion layer: (a) microporous layer for the fresh cathode GDL, (b) microporous layer for the faded cathode GDL, (c) backing layer for the fresh cathode GDL and (d) backing layer for the faded cathode GDL.

anode is resulted from the combined action of the two mentioned water fluxes with opposite direction.

However, with the durability testing time goes on, more water accumulates in the cathode micropores and consequently blocks the transport of oxygen. Thus the current density in the durability test decreased gradually, which results in smaller ORR water and electro-osmotic water. Naturally, water activity on the interface of membrane and cathode catalyst layer will be smaller, leading to gradually strengthened diffusion of water from anode to cathode. Additionally, the residual water in the cathode will reduce the hydrophobicity of the cathode GDL as the hydrophobic micropores are gradually filled with water, which contributes to the lowered hydraulic pressure in the cathode. Therefore, the counter water flux driven by hydraulic pressure difference becomes weaker. Based on the detailed analysis above, it can be conclude that total water transported by diffusion from anode to cathode becomes larger and finally a reversed and positive diffusion flux is obtained at 446 h.

As for the last measurement on water collection, the total diffusive water flux is from cathode to anode again, which happens after "cathode blowing". This is probably caused by the draining away of the accumulated water from the hydrophobic micropores, which results in not only the increased liquid/gas interface, but also the effective oxygen transport and consequently the increase of water activity in the cathode. Thus the backflow water generated from the cathode capillary force increases and the water driven by concentration gradient from anode to cathode decreases at the meanwhile, resulting in the negative value of the total diffusion flux. However, the significant reduction for the collected water, as shown in Fig. 3, might be resulted from the irreversible structural change of the cathode GDL.

3.3. Irreversible degradation of the cathode GDL

CO-stripping curves of the anode catalyst layer and CV curves of the cathode catalyst layer before and after the durability test are shown in Fig. 5. The calculated ECA values are also listed in the figure. It can be seen clearly that ECA reduces in both catalyst layers after the durability test, which leads to the irreversible degradation of the durability performance. In addition to the electro-catalysts degradation, the variation of the microstructure and the hydrophobicity for the cathode GDL is another key factor resulting in the deterioration of the durability performance.

The morphological comparisons between the fresh and faded MPL obtained from SEM are shown in Fig. 6. For the MPL, slight change can be observed. Fig. 6(a) shows that nearly all the carbon fibers are covered with carbon powder and PTFE particles, and some small cracks are observed for the fresh one. While more carbon fibers appear in the faded one as shown in Fig. 6(b). In addition, lots of micropores in the scale between 50 and 100 μm are formed on the MPL surface after the durability test. As for the backing layer of the cathode GDL, the fresh one clearly reveals its carbon fiber structure in Fig. 6(c). While evident viscous materials attached to the carbon fibers are observed in the faded backing layer as displayed in Fig. 6(d). Moreover, the micropores formed with carbon fiber becomes less and smaller after the 600 h durability test.

The contact angle comparison for the cathode GDL before and after the durability test is shown in Fig. 7. It is 7.5° smaller after the 600 h operation than the one before the durability test for MPL, whereas the contact angle of the backing layer increases by 3.5° in the same period. Furthermore, the value of the MPL for fresh GDL is larger than that of the backing layer, which could certainly form a hydrophobic gradient. But the variation of the hydrophobic

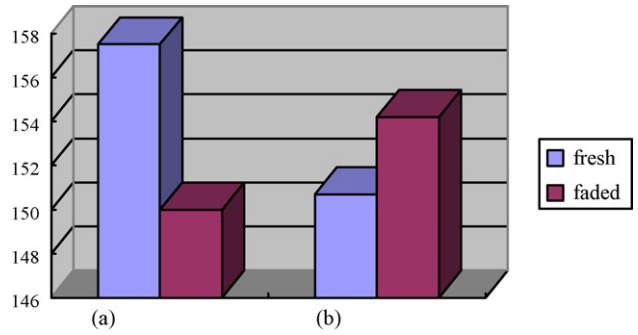

Fig. 7. Comparison of the contact angle for the fresh and faded cathode gas diffusion layers: (a) microporous layer and (b) backing layer.

properties after the durability test makes this gradient reversed. Fig. 8 displays EDX spectra for the fresh and faded cathode GDLs. The analytical results of F/C atomic ratio are listed in Table 2. The F/C atomic ratio for the MPL of the fresh GDL is 0.173, which decreases to 0.157 after 600 h operation. In contrast, it increases

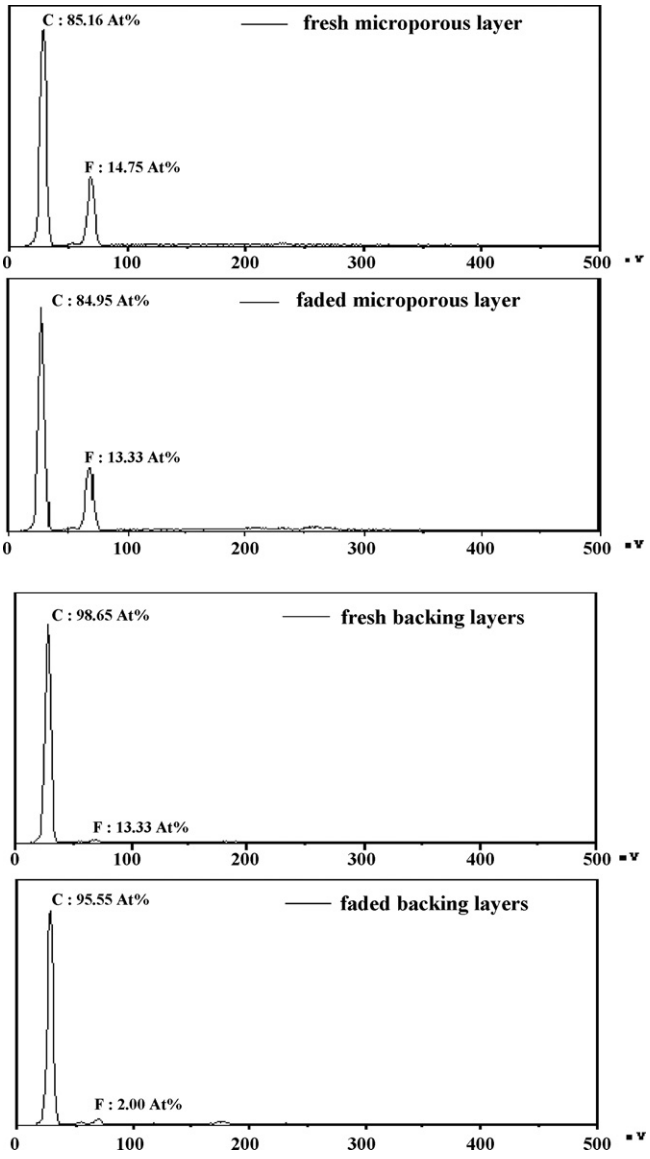

Fig. 8. EDX spectra for the fresh and faded cathode gas diffusion layer.

Table 2
Comparison of the atomic ratio of F/C for the cathode GDL from EDX.

	Microporous layer	Backing layer
Fresh cathode GDL	0.173	0.0135
Faded cathode GDL	0.157	0.0209

from 0.0135 to 0.0209 for the BL during that time. Since PTFE is added to the ink of the microporous layer, fluorine detected by the EDX should come from it. Therefore, the changes of F/C atomic ratio could imply the variation of the hydrophobic properties due to the strong hydrophobicity of PTFE [25]. These results are in good agreement with the previous contact angle analysis.

Based on these results, it is obvious that the changes of the microsructure and hydrophobicity should contribute to the significant reduction of the removal water and the decrease of the over-all cell performance after the durability test. Firstly, the weakened hydrophobicity and the slightly increased size of the micropores in the MPL would result in a decreased capillary pressure and consequently the reduction of the backflow water ability. Furthermore, the increased hydrophobicity as well as the decreased size of the micropores in cathode backing layer would hinder water remove away from MPL to BL, which aggravated the difficulty of water releasing from the cathode GDL [26]. Therefore, more water is likely to accumulate in the cathode, which affects the water management of the cathode GDL and consequently results in "cathode flooding" and over-all cell performance deterioration as shown in Fig. 2.

4. Conclusion

In this work, the correlation of water transport and cell performance was studied by analyzing water transport through the membrane during a 600 h durability test. It was found that the quantity of water produced by diffusion was the key factor that affects the cell durability. With the testing time goes on, the capillary pressure weakened, and the water flux produced by hydraulic pressure difference reduced, which would consequently make the cell durability deteriorate.

Furthermore, "cathode blowing" with dry air under a small flow rate for 150 h was applied to remove the majority of the residual water in the cathode GDL. Experimental results showed that the cell performance recovered partially due to the recovery of the water transport ability in the cathode GDL.

In addition, the contact angle, SEM and EDX analysis of the cathode GDL were used to investigate the material characteristics during the durability test. Results indicated that the variation of the hydrophobicity and the surface morphology in the MPL and backing layer affected the water management ability and the cell performance severely.

Acknowledgements

This work was financially supported by Innovation Foundation of Chinese Academy of Science (K2006D5), Hi-Tech Research and Development Program of China (2006AA05Z137, 2006AA05Z139) and National Natural Science Foundation of China (Grant No.: 20776139).

References

[1] S.S. Kocha, in: W. Vielstich, A. Lamm, H. Gasteiger (Eds.), Handbook of Fuel Cell-Fundamentals Technology and Applications, vol. 3, John Wiley & Sons, New York, 2003 (Chapter 43).
[2] C. Lim, C.Y. Wang, Electrochim. Acta 49 (2004) 4149.
[3] X.M. Ren, P. Zelenay, S. Thomas, J. Davey, S. Gottesfeld, J. Power Sources 86 (2000) 111.

[4] H. Kim, S. Shin, Y. Park, J. Song, H. Kim, J. Power Sources 160 (2006) 440.
[5] M.K. Jeon, K.R. Lee, K.S. Oh, D.S. Hong, J.Y. Won, S. Li, S.I. Woo, J. Power Sources 158 (2006) 1344.
[6] X. Cheng, C. Peng, M. You, L. Liu, Y. Zhang, Q.B. Fan, Electrochim. Acta 51 (2006) 4620.
[7] W.M. Chen, G.Q. Sun, J.S. Guo, X.S. Zhao, S.Y. Yan, J. Tian, S.H. Tang, Z.H. Zhou, Q. Xin, Electrochim. Acta 51 (2006) 2391.
[8] L.S. Sarma, C.H. Chen, G.R. Wang, K.L. Hsueh, C.P. Huang, H.S. Sheu, D.G. Liu, J.F. Lee, B.J. Hwang, J. Power Sources 167 (2007) 358.
[9] P. Piela, C. Eickes, E. Brosha, F. Garzon, P. Zelenay, J. Electrochem. Soc. 151 (2004) A2053.
[10] J.G. Liu, Z.H. Zhou, X.S. Zhao, Q. Xin, G.Q. Sun, B.L. Yi, Phys. Chem. Chem. Phys. 6 (2004) 134.
[11] C. Chen, G. Levitin, D.W. Hess, T.F. Fuller, J. Power Sources 169 (2007) 288.
[12] M.K. Jeon, J.Y. Won, K.S. Oh, K.R. Lee, S.I. Woo, Electrochim. Acta 53 (2007) 447.
[13] C.Y. Wang, Chem. Rev. 104 (2004) 4727.
[14] C. Xu, T.S. Zhao, Y.L. He, J. Power Sources 171 (2007) 268.
[15] E. Peled, A. Blum, A. Aharon, M. Philosoph, Y. Lavi, Electrochem. Solid-State Lett. 6 (2003) A268.
[16] F.Q. Liu, G.Q. Lu, C.Y. Wang, J. Electrochem. Soc. 153 (2006) A543.
[17] Q. Mao, G.Q. Sun, S.L. Wang, H. Sun, G.X. Wang, Y. Gao, A.W. Ye, Y. Tian, Q. Xin, Electrochim. Acta 52 (2007) 6763.
[18] G.Q. Lu, F.Q. Liu, C.Y. Wang, Electrochem. Solid-State Lett. 8 (2005) A1.
[19] C. Xu, T.S. Zhao, J. Power Sources 168 (2007) 143.
[20] M.M. Mench, C.Y. Wang, J. Electrochem. Soc. 150 (2003) A79.
[21] C. Eickes, P. Piela, J. Davey, P. Zelenay, J. Electrochem. Soc. 153 (1) (2006) A171.
[22] U. Pasaoqullari, C.Y. Wang, J. Electrochem. Soc. 151 (2004) A399.
[23] N. Nakagawa, M.A. Abdelkareem, K. Sekimoto, J. Power Sources 160 (2006) 105–115.
[24] X.M. Ren, W. Henderson, S. Gottesfeld, J. Electrochem. Soc. 144 (1997) L267.
[25] X.M. Ren, S. Gottesfeld, J. Electrochem. Soc. 148 (2001) A87.
[26] P.K. Sinha, P.P. Mukherjee, C.Y. Wang, J. Mater. Chem. 17 (2007) 3053.